A New Class of Multi-Band Filters Based on The Same Phase Extension Scheme

Xumin Yu *Member*, Xiaohong Tang *Member, IEEE*, Fei Xiao, *Member, IEEE,* and Xinyang He

***Abstract*—This paper presents a new class of Multi-band filters based on same phase extension scheme, in which each channel is dedicated to selected band and center frequency by using the scheme of same phase extension. The equivalent circuit is the combination of multi-inline networks connected with two manifold waveguides, the structure of which has the same phase extension. The advantage of this method is that each in line network represents an individual channel. A dual-mode tri-band filter is measured and described.**

***Index Terms*—Band-pass filter, manifold waveguide, multi-band, resonator filter.**

I. Introduction

Microwave multiband filters have been attracting considerable attention [1]-[6]. Recent designs of these types of filters, which generate transmission zeros between the bands, involve cross-coupled resonators, as in the single-band case. The shortage of coupling schemes is that the sensitivity of the individual pass-bands to manufacturing errors is connected with the whole order of the filters, but not with the individual bands. A dual-mode dual-band filter was introduced in [7]. In that filter, each individual band is controlled by a dedicated polarization of the dual-mode resonators, and a transmission zero is increased to improve the rejection of two bands. However, such an approach can not present more pass-bands filters.

In this paper, we propose a new design of multi-band filter, in which each individual band is controlled by a dedicated channel. The manifold-coupled approach, which is a kind of same phase extension scheme, is used to connect each channel's input and output ports. This kind of multiband filter requires the presence of all channel filters at the same time so that the effect of channel interactions can be compensated in the designed process. The manifold itself is a transmission line, such as a coaxial line, a rectangular waveguide, or some other low-loss structure. It is possible to achieve a channel performance in the manifold-coupled configuration, which is close to the one that can be obtained from a channel filter by itself. As an example, a dual-mode tri-band filter is designed and presented.

II. Theory and Equivalent Circuit

The equivalent circuits of multiband filters are parallel circuits. In the microwave field, the ideal parallel circuits must meet two requirments. One is the common point of parallel circuits has a common pass power for every frequency in the pass-band; the other is that the point also has a common phase for every frequency in the pass-band. In order to design the ideal common point in parallel circuits, a piece of metal, the area of which is as small as possible, will be used generally. In other transmission structures, the more compact the structure of common part is, the better the achieved performance of common point is. However, when the parallel circuits increase, the design of the common point becomes more difficult.

A manifold-coupled multiplexer, which is capable of realizing optimum performance for absolute insertion loss、amplitude and group delay response, has been known for decades [8]-[13]. The manifold-coupled approach is a scheme of the common point for more parallel circuits. Using this method, the common port of each parallel circuit can share the same phase at pass-band frequencies by carefully designing. The power differences of common port, which may be due to different transmission ways, are too small to be ignored. The same technology with careful arrangements can be used to design robust manifold-coupled multi-band filters.

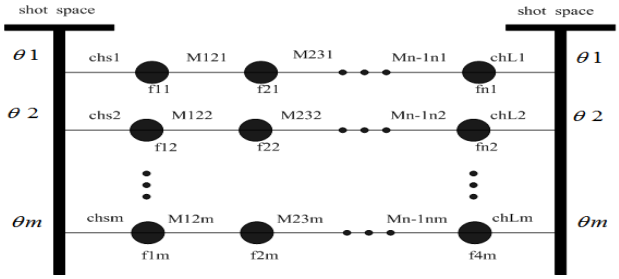

Fig.1. The equivalent circuit of m-band n-order filters

The equivalent circuit of this class of filters, in terms of inverters and resonators, consists of *m* non-interacting paths connected with two manifold transmission lines, as shown in Fig.1. If n cavities are used, each path contains n resonators that are directly coupled by inverters. The *m* paths are connected to the input and output nodes with manifold. Each channel can be designed separately. Naturally, this equivalent circuit is valid for the pass-bands just like a manifold multiplexer. A specific response yielded by the extraction of the parameters of the equivalent circuit in Fig.1 can be carried out by optimization, which is the same as a manifold multiplexer in [11].

As an example, a six-cavity three-band filter with the following specifications, 40 MHz, 60 MHz and 100 MHz centered at 14 GHz, 14.11 GHz and 14.28 GHz, is presented. The in-band return loss in three pass-bands is 20 dB. The three

bands are separated by two transmission-zero at 14.047 GHz and 14.2455 GHz. The initial coupling matrix of channel filter is obtained:

$$M = \begin{bmatrix} 0 & 1.2 & 0 & 0 & 0 & 0 \\ 1.2 & 0 & 0.98 & 0 & 0 & 0 \\ 0 & 0.98 & 0 & 0.745 & 0 & 0 \\ 0 & 0 & 0.745 & 0 & 0.98 & 0 \\ 0 & 0 & 0 & 0.98 & 0 & 1.2 \\ 0 & 0 & 0 & 0 & 1.2 & 0 \end{bmatrix} \quad (1)$$

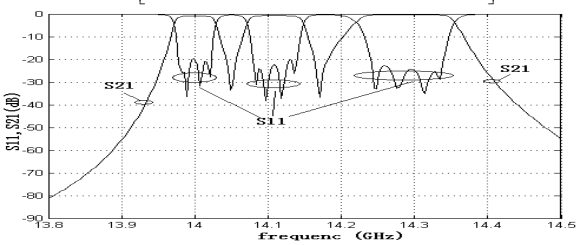

Fig.2. Response of the whole filter circuit (Q=8000)

After connecting the whole channels with manifold by cascading these net [ABCD] matrices of each section in the structure, the response of this filter is shown in Fig.2.The unloading Q 8000 is assumed. All the specifications are met.

III. FILTER STRUCTURES

Compared with a manifold-coupled multiplexer shown in Fig.3, a manifold-coupled multiband filter's approach shown in Fig.4 is viewed as one more manifold to connect each channel's output.

The most important requirement in this configuration is to preserve realizability in the whole structure. The two designed manifold transmission lines can be connected with each channel's input and output smoothly. The channel filter in this paper (Fig.5) can be designed based on the dual-mode or single-mode channels, which have the same length L. Every channel has two cylindrical cavities and two sub rectangular waveguides, which have been carefully designed.

For the structure in Fig.6, the resonators are uniform sections of a cylindrical waveguide in which a coupling screw and two frequency tuning screws are placed in the middle of the cavity. There is a coupling aperture between two cavities. This cylindrical dual-mode configuration channel was used to design output multiplexer in [12]. From this type of channel filter, it is able to gain high Q, low insertion loss, small size and cross-coupled resonators.

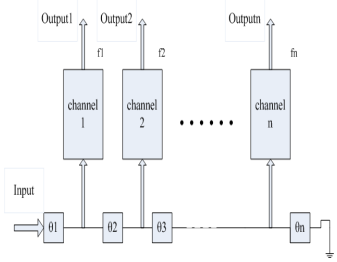

Fig.3.Manifold-coupled multiplexer

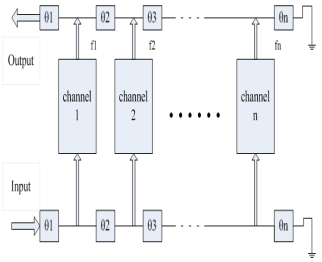

Fig.4.Manifold-coupled multiband filter

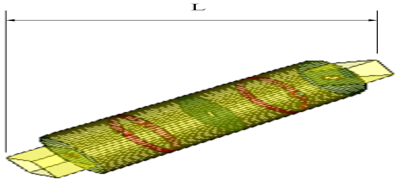

Fig.5. One channel of the proposed manifold-coupled dual-mode multi-band filter

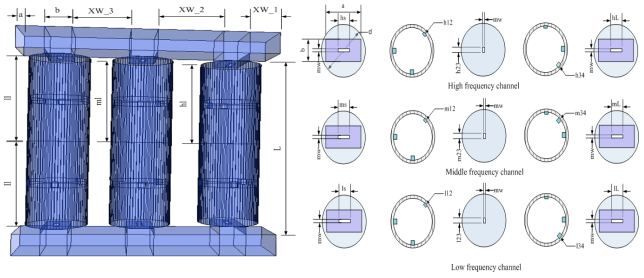

a b

Fig.6 The size of tri-bands filter (a. Layout of the proposed manifold-coupled dual-mode multiband filter; b. Coupling structures of three channels in the proposed manifold-coupled dual-mode multiband filter)

IV. DESIGN

The design approach used in this paper is perfectly illustrated by the structure in Fig.6 as an example. All the channel filters are electrically connected to each other through the near-loss-less manifold waveguide. The design consists in implementing the equivalent circuit in Fig.1. The manifold multi-band filters need to be considered as a whole, and thus optimization method has been utilized to achieve the final design. To speed up the overall optimization, it is efficient to analyze each channel's input/output to common port transfer characteristic individually, and the common port return loss.

A. Common Port Return Loss

In the multi-band filters, the input and output are common port of all channels. The manifold in this paper is the waveguide, and the junctions are *E*-plane. The junctions are best characterized with three-port *S* parameters, and symmetry of junctions about the vertical axis in Fig.7, $S11 = S22$ and $S32 = -S31$. The S-parameter matrices are calculated by assuming a matched termination at each port. When the termination at one port is arbitrary, the two-port S parameters between the others can be defined using the following formula.

1) Admittance Y_{L2} *(≠1) at port 2:*

$$\begin{bmatrix} S'_{11} & S'_{31} \\ S'_{31} & S'_{33} \end{bmatrix} = \begin{bmatrix} S_{11} & S_{13} \\ S_{31} & S_{33} \end{bmatrix} + \frac{\Gamma_2}{1-\Gamma_2 S_{11}} \begin{bmatrix} S_{21}^2 & kS_{21}S_{31} \\ kS_{21}S_{31} & S_{31}^2 \end{bmatrix} \quad (2)$$

, where $\Gamma_2 = (1-Y_{L2})/(1-Y_{L2})$ and Y_{L2} is the admittance at port 2 of the junction and $k = -1$ for *E*-plane junctions. This modified S matrix can also be applied, if Y_{L1} is terminating port 1.

2) Admittance Y_{L3} *(≠1) at port 3:*

$$\begin{bmatrix} S'_{11} & S'_{12} \\ S'_{21} & S_{22} \end{bmatrix} = \begin{bmatrix} S_{11} & S_{12} \\ S_{21} & S_{22} \end{bmatrix} + \frac{\Gamma_3 S_{21}^2}{1-\Gamma_3 S_{22}} \begin{bmatrix} 1 & k \\ k & 1 \end{bmatrix} \quad (3)$$

, where $\Gamma_3 = (1-Y_{L3})/(1-Y_{L3})$ and Y_{L3} is the admittance at port 3 of the junction and $k = -1$.

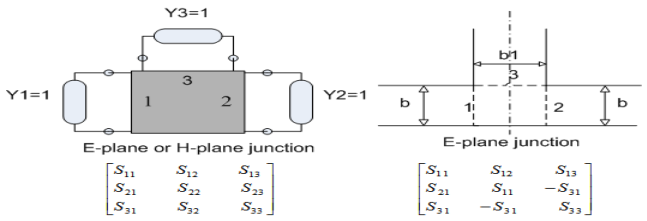

Fig.7. E-plane waveguide junction and S-parameter matrix representation

The channel filter input admittances Y_{F1}, Y_{F2} and Y_{F3} are determined at the frequency points in the band rang. The new S parameters of each junction are calculated using (3). These new S parameters are converted to [ABCD] and cascaded in manifold structure with θ_{M1} , θ_{M2} and θ_{M3} . The along-manifold admittances Y_{M1}, Y_{M2} and Y_{M3} are obtained as shown in Fig.8

$$Y_{Mi} = \frac{1+S_{11i}}{1-S_{11i}} \quad \ldots\ldots (4)$$

, where i =1, 2…, $n+1$, and n is the number of channels on the manifold. The CPRL (Common port return loss) can be obtained from the final admittance Y_{M4} as shown in Fig.8.

$$RL_{CP} = -20\log_{10}\frac{1+Y_{Mn+1}}{1-Y_{Mn+1}}(dB) \quad \ldots\ldots (5)$$

When the Y_{F2} , and Y_{F3} are determined, θ_{M1}, θ_{M2} and θ_{M3} are optimized to generate better CPRL. In this scheme, it implies that the symmetry structure of each channel may be more easily designed. However, in order to obtain the transmission zero between bands, asymmetry structure needs to be used in dual-mode cavities.

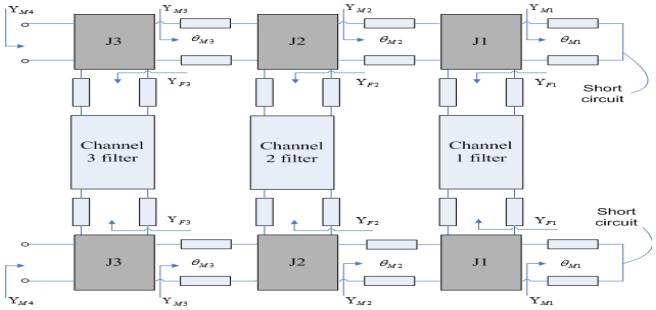

Fig.8. The design of common ports return loss.

B. *Channel Filter Design*

Generally, each band of multi-band filters is widely spaced, although they react with each other through the manifold directly. The channel interactions are not high. The doubly terminated networks are used to design the channel filter. In this paper, three doubly terminated filters are designed for three channels before optimization.

As shown in Fig.6, two coupling screws in each channel are used to realize *M12* and *M34* in the coupling matrix, the inter-cavity rectangle coupling iris realizes *M23*, and the rectangle coupling irises between cylindrical and rectangle waveguide realize the *M01* and *M45*, respectively. The high and low frequency channels have the same corresponding coupling-routing diagram. Only one coupling screw of the middle frequency channel turns 90 ° to obtain the two transmission zeros.

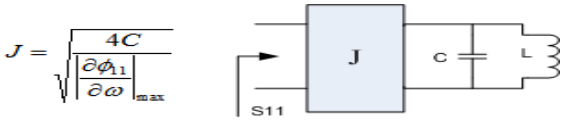

Fig.9. The circuit representing a closed cavity is used to design the input and output coupling coefficient.

The design of input/output coupling irises for each channel is done by simulating a single closed cavity coupled to the input/output manifold waveguide. The coupling coefficients, which are the result of optimization, are related to the maximum of the derivative of the phase of *S11* with respect to frequency [9]. The relationship between the derivative of the phase of the reflection coefficient and the input/output coupling coefficients can be established by using the circuit in Fig.9. The coupling coefficient is given by [9].

The electromagnetic simulation structure and equivalent circuit of inter-cavity coupling irises are shown in Fig.10. The equivalent circuit parameters can be obtained directly from the S-parameters though (6). The normalized coupling coefficients and the angle ϕ are given in (7) as follows:

$$jX_s = \frac{1-S_{21}+S_{11}}{1-S_{11}+S_{21}} \qquad jX_p = \frac{2S_{21}}{(1-S_{11})^2 - S_{21}^2} \qquad (6)$$

$$\phi = -\tan^{-1}(2X_p + X_s) - \tan^{-1}(X_s)$$

$$K = \left|\tan\left(\phi/2 + \tan^{-1}(X_s)\right)\right| \qquad (7)$$

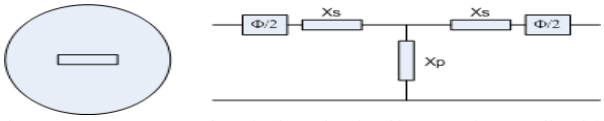

Fig.10. EM structure and equivalent circuit of inter-cavity coupling irises.

The coupling screws can be designed in the same way. The length of resonators is half a guided wavelength at the designed frequency and they are corrected by a phase term to account for the loading by the irises and screws. The actual lengths are related to ϕ_i of irises and screws, which is given in (8) as follows.

$$L_i = \frac{\lambda_g}{2\pi}\left(\pi - \frac{1}{2}(\phi_i + \phi_{i+1})\right) \qquad (8)$$

V. Applications And Results

To illustrate the design procedure, a four-cavity dual-mode three-band filter was designed and optimized. The filter has three bands: 13.98 GHz-14.02 GHz, 14.08 GHz-14.14 GHz and 14.24 GHz-14.34 GHz. The in-band return loss is approximate 20 dB.

The initial coupling matrix of one channel is given in (1) and the final response of the whole filter is given in Fig.2. The initial design was optimized by using Mician's commercial software package μ Wave Wizard. The response of the optimized structure is shown in Fig.11. The transmission zero outside of the pass-band is generated by cross coupling structure in the channel filter itself. The dimensions of the optimized filter are a=19.05 mm, b=9.525 mm, d=22.5 mm, mw=2 mm, L=72 mm, XW_1=20.9847 mm, XW_2=23.6211 mm, XW_3=11.0616 mm, ll=17.9165 mm, ml=17.683 mm, hl=17.2155 mm, ls=6.6346 mm, l23=3.3238 mm, ll=6.5667 mm, ms=7.0559 mm, m23=4.12 mm, ml=6.942 mm,

hs=7.5396 mm, h23=5.0122 mm, and hl=7.459 mm. The iris thickness is t=0.5 mm.

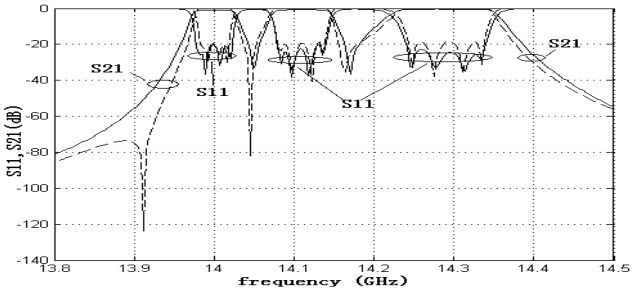

Fig.11. Response of optimized four-cavity three-band dual-mode filter. Dashed lines: EM simulation from Mician's μ Wave Wizard. Solid lines: ideal response.

VI. Sensitivity Analysis

The investigation of the design's sensitivity to errors in the dimensions of the structure is an important step for designing microwave filters, prior to fabrication. The filters' dimensions in Fig.6. are randomly changed by ± 0.025mm, and the resulting responses are plotted together in Fig.14. For each channel with its own structure, the sensitivity of each band is very similar to a single filter. Since the manifold waveguide connects the input and output of each channel, the dimensions of manifold waveguide is more sensitive to affecting each channel. The low narrow band shows more sensitivity of frequency than the other bands do, just like a narrow band filter. The more width the designed pass-band is, the less sensitivity it shows.

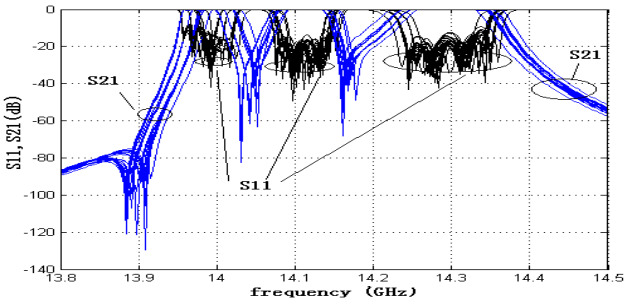

Fig.12. Sensitivity analysis of the tri-band dual-mode filter

VII. Measurement

The measured result of a dual-mode tri-bands filter has been shown in fig.13. The filter has three bands: 13.98GHz-14.01 GHz, 14.09 GHz-14.15 GHz and 14.25 GHz-14.35 GHz. Two transmission zeros are generated along the three bands. The photo of the dual-mode tri-bands filter has been shown in fig.14. The presented filter is a litter different from the simulated one, which is caused by error of processing and debugging. However, the measured result, that confirms the same phase extension scheme, is useful for multi-band filter implementing.

VIII. Conclusion

This paper presents a new class of Multi-band filters, in which each channel is dedicated to selected band and center frequency by using the scheme of same phase extension. Two common manifold waveguides are used to connect several separate channels. This implies that each channel models an individual filter, which can present a straight-forward initial design. The advantage of same phase extension is that it is a kind of method to implement common point in parallel circuits. In the filter, a transmission zero between two pass-bands is generated by adjusting a coupling screw of one channel. Simulation result and sensitivity analysis have been elucidated. The lowest band of measured result is narrow than that of simulated result due to error of processing and debugging. However, the measured result, that confirms the same phase extension scheme, is useful for multiband filter implementing, either. Designs, in which the structure of resonator and manifold transmission line are different, are also possible.

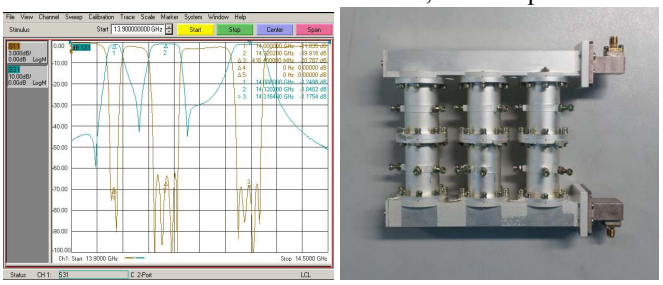

a b

Fig.13. Measured response and Photo dual-mode tri-bands filter(a.Measured response; b. Photo)

References

[1] G. Macchiarella and S. Tamiazzo, "Design techniques for dual-pass-band filters," *IEEE Trans. Microw. Theory Tech.,* vol. 53, no.11, pp. 3265-3271, Nov. 2005.

[2] M. Mokhtaari, J. Bornemann, K. Rambabu, and S. Amari, "coupling matrix design of dual and triple passband filters," *IEEE Trans. Microw. Theory Tech.,* vol.55, no. 11, pp. 3940-3946, Nov. 2006.

[3] V. Lunot, F. Seyfert, S. Bila, and A. Nasser, "Certified computation of optimal multiband filtering functions," *IEEE Trans. Microw. Theory Tech.,* vol. 56, no. 1, pp. 105-112, Jan. 2008.

[4] P. Lenoir, S. Bila, F. Seyfert, D. Baillargeat, and S. Verdeyme, "Synthesis and design of asymmetrical dual-band bandpass filters based on equivalent network simplification," *IEEE Trans. Microw. Theory Tech.,* vol. 54, no. 7, pp. 3090-3097, Jul. 2006.

[5] G. Macchiarella and S. Tamiazzo," Dual-band filters for base station multi-band combiners," in *IEEE MTT-S Int. Microw. Symp. Dig*., Jun. 2007, pp. 1289-1292.

[6] Y. Zhang, K. A. Zaki, J. A. Ruiz-Cruz, and A. E. Atia, "Analytical synthesis of generalized multi-band microwave filters," in *IEEE MTT-S Int. Microw. Symp. Dig.,* Jun. 2007, pp. 1273-1276.

[7] S. Amari, and M. Bekheit, "A new class of dual-mode dual-band waveguide filters," *IEEE Trans. Microw. Theory Tech.,* vol. 56, no. 8, pp. 1938-1944, Nov. 2008.

[8] J. D. Rhodes and R. Levy, "Design of general manifold multiplexers," *IEEE Trans. Microwave Theory Tech.* MTT-27, 111-123 (1979).

[9] J. D. Rhodes and R. Levy, "A generalized multiplexer theory," *IEEE Trans. Microwave Theory Tech.* MTT-27, 99-110 (1979).

[10] C. Kudsia, R. Cameron, and W. C. Tang, "Innovation in microwave fiters and multiplexing network for communication satellite systems, *IEEE Trans. Microwave Theory Tech.* MTT-40, Jun. 1992, pp. 1133-1149.

[11] J. Bandler, R. Biernacki, S. Chen, P. Grobelny, and R. Hemmers, Space mapping technique for electromagnetic optimization, *IEEE Trans. Microwave Theory Tech.* MTT-42, Dec. 1994, pp. 2536-2544.

[12] R. J. Cameron, C. M. Kudsia, and R. R. Mansour, *Microwave filters for communication systems*. Chapter 18 New Jersey, U.S.: WILEY Press, 2007.

[13] J. Bandler, S. Daijavad, and Q.-J. Zhang, "Exact simulation and sensitivity analysis of multiplexing networks," *IEEE Trans. Microwave Theory Tech.* MTT-34, Jan. 1986, pp. 102-111.